

Learning How to Dynamically Route Autonomous Vehicles on Shared Roads

Daniel A. Lazar*, Erdem Bıyık*, Dorsa Sadigh, and Ramtin Pedarsani,

Abstract—Road congestion induces significant costs across the world, and road network disturbances, such as traffic accidents, can cause highly congested traffic patterns. If a planner had control over the routing of all vehicles in the network, they could easily reverse this effect. In a more realistic scenario, we consider a planner that controls autonomous cars, which are a fraction of all present cars. We study a dynamic routing game, in which the route choices of autonomous cars can be controlled and the human drivers react selfishly and dynamically to autonomous cars’ actions. As the problem is prohibitively large, we use deep reinforcement learning to learn a policy for controlling the autonomous vehicles. This policy influences human drivers to route themselves in such a way that minimizes congestion on the network. To gauge the effectiveness of our learned policies, we establish theoretical results characterizing equilibria on a network of parallel roads and empirically compare the learned policy results with best possible equilibria. Moreover, we show that in the absence of these policies, high demands and network perturbations would result in large congestion, whereas using the policy greatly decreases the travel times by minimizing the congestion. To the best of our knowledge, this is the first work that employs deep reinforcement learning to reduce congestion by influencing humans’ routing decisions in mixed-autonomy traffic.

I. INTRODUCTION

CONGESTION can result in substantial economic and social costs [1] which have only been growing in recent years, especially with the advent of ride-hailing services [2]. Congestion is formed by a number of mechanisms, such as when many vehicles try to enter a road at the same time. A higher-level cause is from how people choose their routes – when people selfishly choose the quickest routes available to them, this often results in greater congestion and longer travel time than if people had their routes chosen for them optimally in terms of the overall experienced delay [3]. There are some existing methods for fighting congestion, such as congestion pricing [4], variable speed limits [5] and highway ramp metering [6]. However, they can be difficult to administer, and can require significant changes to infrastructure.

The introduction of autonomous vehicles to public roads provides an opportunity for better congestion management. Our key idea is that by controlling the routing of autonomous vehicles, we can change the delay associated with traversing each road, thereby indirectly influencing peoples’ routing choices. By influencing people to use more “socially advantageous” routes, we can eliminate long queues and significantly reduce traffic jams on roads.

* Authors contributed equally.

Daniel A. Lazar and Ramtin Pedarsani are with the Department of Electrical and Computer Engineering, UC Santa Barbara, CA, 93106 USA e-mail: {dlazar,ramtin}@ucsb.edu.

Erdem Bıyık is with Department of Electrical Engineering, Stanford University, CA, 94305 USA e-mail: ebiyik@stanford.edu.

Dorsa Sadigh is with Department of Computer Science and Department of Electrical Engineering, Stanford University, CA, 94305 USA e-mail: dorsa@cs.stanford.edu.

The model for *mixed-autonomy* traffic, meaning traffic with both human-driven and autonomous vehicles, is complex, involving very large and continuous state space and continuous action space. Having human drivers dynamically respond to the choices of the autonomous vehicles further complicates the matter, making a dynamic programming-based approach and other classical methods infeasible. Because of this, we use deep reinforcement learning (RL) to learn a policy. Specifically, we show it is possible to learn a policy via proximal policy optimization (PPO) [7] that mitigates traffic congestion by managing routing of autonomous cars given the network state.

To understand the performance of the learned policy, we investigate the *equilibrium* behavior of the network. Previous works [8], [9] have shown that there is a wide spectrum of equilibria in traffic networks, meaning situations in which everyone is taking the quickest route immediately available to them, and these equilibria can have greatly varying average user delay. We establish efficient ways to compute equilibria in the network and compare the best equilibrium (in terms of latency) with the RL policy, which works regardless of whether equilibrium conditions hold or not. We show that the learned policy reaches the ‘desirable’ equilibria that have low travel times when starting with varying traffic patterns, and can recover network functionality after a disturbance such as a traffic accident.

Our contributions are as follows:

- *Vehicle flow and choice modeling*: We formalize a traffic model that extends the classic Cell Transmission Model (CTM) [10] to characterize vehicle flow on parallel shared roads. We adopt log-linear learning to model how people update their routing choices as traffic states change.
- *Finding a control policy via deep RL*: We employ deep RL methods to learn a routing policy for autonomous cars that effectively saves the traffic network from unboundedly large delays.
- *Theoretical analysis*: We characterize equilibria in the network and derive a polynomial-time computation for finding optimal equilibria. We show that the RL control policy is able to bring our network state to the best possible equilibrium when starting from a congested equilibrium or after a network disturbance.

We visualize our framework as a schematic diagram in Fig. 1 and preview our results in Fig. 2, showing that the RL policy successfully stabilizes queues in the traffic which would otherwise be congested.

Literature review. Many works seek to understand how much traffic network latency could be improved if vehicle routing was controlled by a central planner, including works on *congestion games* [3], [11]–[14]. Some study how indirectly influencing peoples’ routing choices by providing them network

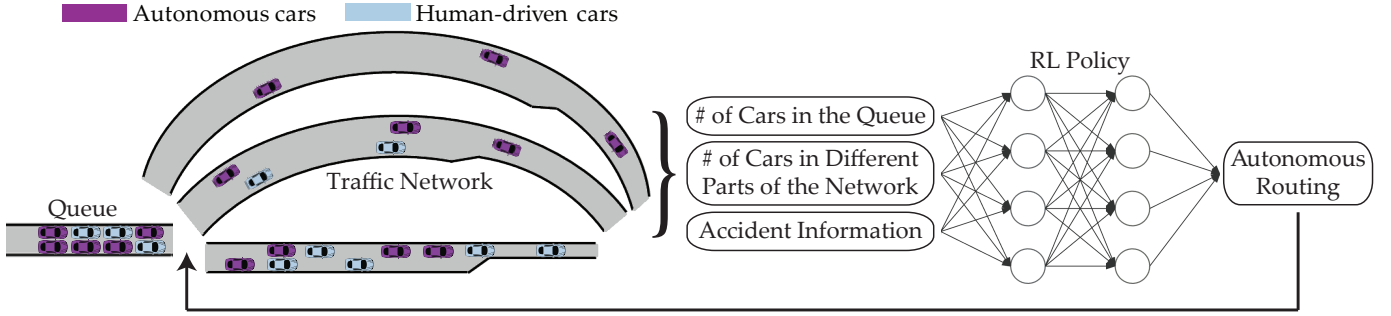


Fig. 1: The schematic diagram of our framework. Our deep RL agent processes the state of the traffic and outputs a control policy for autonomous cars’ routing.

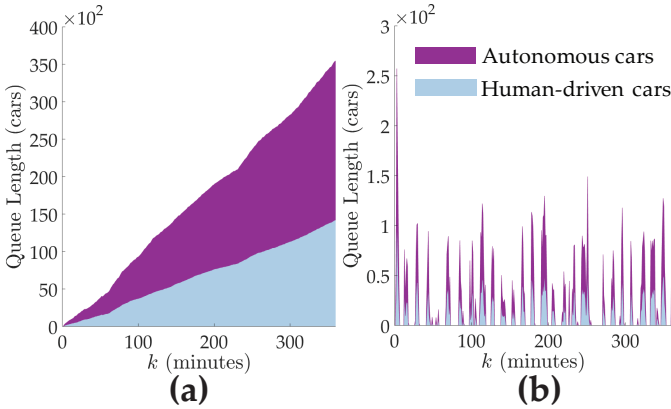


Fig. 2: **(a)** The traffic queue grows linearly when all vehicles try to minimize their travel time, whereas **(b)** RL control of autonomous cars stabilizes this queue (note the scales).

state information affects network performance [15], [16]. *Stackelberg Routing*, in which only some of the vehicles are controlled, is another way to influence routing [17], [18]; some works incorporate the *dynamics* of human routing choices [19]. While providing useful techniques for analysis, the congestion game framework does not reflect a fundamental empirical understanding about vehicle flow on roads, namely that roads with low vehicle density have a roughly constant latency, and roads with high density see latency *increase* as flow *decreases*.

Works on CTM [10], [20] capture this phenomenon, including works that characterize equilibria on roads described with CTM [6]. Notably, some consider equilibria, but not dynamics, of parallel-road Stackelberg Games, including with mixed autonomy [8], [9].

Some works look at the low-level control of autonomous vehicles, specifically how to control their acceleration to smooth traffic flow and ease congestion at bottlenecks [21], [22]; [23] provides a benchmark for gauging the performance of these techniques. Other works learn ramp metering policies [23] and model lane-change behavior with a neural net [24].

II. VEHICLE FLOW DYNAMICS: MODELING ROADS

In this section we describe dynamics governing how vehicle flow travels on a road. We extend the CTM, a widely used model that discretizes roads into *cells*, each with uniform density [10], [20], for mixed-autonomy traffic. In CTM, each road segment has a maximum flow that can traverse it. The

key idea of our extension is that since autonomous vehicles can keep a shorter headway (distance to the car in front of it), the greater the fraction of autonomous vehicles on a road, the greater the maximum flow that the road can serve [9]. Accordingly, our extension lies in the dependence of cell parameters on the *autonomy level*, or the fraction of autonomous vehicles, in each cell.

Consider a road, or path, p , composed of I_p cells. Each cell i has the following parameters: free-flow velocity $\bar{v}_{p,i}$, headway for human driven cars (resp. autonomous cars) traveling at the free-flow velocity $h_{p,i}^h$ (resp. $h_{p,i}^a$) with units cells/vehicle, and number of lanes $b_{p,i}$.

Each cell also has a vehicle density, or number of vehicles on it, $n_{p,i} = n_{p,i}^h + n_{p,i}^a$, where $n_{p,i}^h$ and $n_{p,i}^a$ are, respectively, the number of human-driven and autonomous vehicles. As the cells are much larger compared to the vehicles, we consider these quantities to be continuous variables. Let $\alpha_{p,i} = n_{p,i}^a / (n_{p,i}^h + n_{p,i}^a) \in [0, 1]$ denote the *autonomy level*, or the fraction of autonomous vehicles.

In the CTM, there are two regimes for vehicle flow: free-flow, in which the cell density is less than some *critical density*, and the congested regime, in which the cell density is greater than the critical density but less than the *jam density*. The jam density is the density at which traffic completely stops, denoted the $\bar{n}_{p,i}$. As in [9], [14], [25], [26] and represented in Fig. 3 (a), we model¹ the critical density as $\tilde{n}_{p,i}(\alpha_{p,i}) := b_{p,i} / (\alpha_{p,i} h_{p,i}^a + (1 - \alpha_{p,i}) h_{p,i}^h)$.

There are three factors that can limit the flow from one cell to another. One is the *capacity*, or maximum flow out of a cell, which is the flow of vehicles that traverse the cell at the critical density:

$$\bar{F}_{p,i}(\alpha_{p,i}) := \bar{v}_{p,i} \tilde{n}_{p,i}(\alpha_{p,i}). \quad (1)$$

The flow out of a cell is also limited by the demand in the cell, $\bar{v}_{p,i} n_{p,i}$. The flow entering a cell is limited by that cell’s supply, $(\bar{n}_{p,i} - n_{p,i}) w_{p,i}(\alpha_{p,i})$, where $w_{p,i}$, the *shockwave speed*, is $w_{p,i}(\alpha_{p,i}) := \bar{v}_{p,i} \tilde{n}_{p,i}(\alpha_{p,i}) / (\bar{n}_{p,i} - \tilde{n}_{p,i}(\alpha_{p,i}))$.

Combining these, we denote the flow from cell $i-1$ to cell i on path p as $f_{p,i-1}$. As shown in Fig. 3 (b),

$$f_{p,i-1} := \min(\bar{v}_{p,i-1} n_{p,i-1}, (\bar{n}_{p,i} - n_{p,i}) w_{p,i}(\alpha_{p,i}), \bar{F}_{p,i-1}(\alpha_{p,i-1})). \quad (2)$$

¹In this model, autonomous vehicles can follow any vehicle with headway h_p^a , regardless of the type of vehicle it is following, or autonomous vehicles can rearrange themselves to form platoons as in [27].

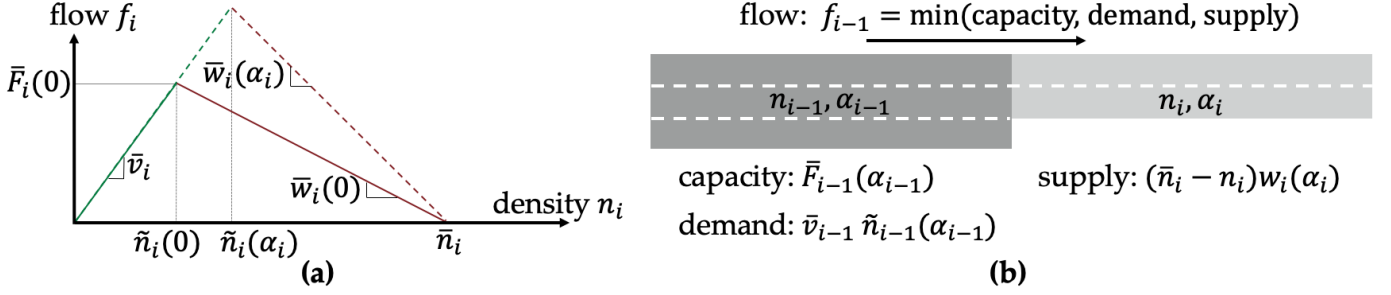


Fig. 3: **(a)** Fundamental diagram of traffic governing vehicle flow in each cell of the Cell Transmission Model. The solid line corresponds to a road with only human-driven vehicles; the dashed line represents a road with both vehicle types at autonomy level α_i . Green and red respectively represent a road in free-flow and congestion. **(b)** The flow from one cell to another is a function of the density n and autonomy level α in each cell. In both figures, we suppress the notation for path p .

We consider no capacity limit for vehicles entering a road and no supply limit for vehicles exiting a road. We use $f_{p,0}$ to denote the flow entering path p and require that $f_{p,0} \leq (\bar{n}_{p,1} - n_{p,1})w_{p,1}(\alpha_{p,1})$. Similarly, the flow exiting a road is $f_{p,I_p} := \min(\bar{v}_p n_{p,I_p}, \bar{F}_{p,I_p}(\alpha_{p,I_p}))$.

Putting this together, we describe the dynamical system (transition model of density of each cell on each path) as follows, where k denotes the time index.

$$\begin{aligned}
 n_{p,i}^h(k+1) &= \\
 & n_{p,i}^h(k) + (1 - \alpha_{p,i-1}(k))f_{p,i-1}(k) - (1 - \alpha_{p,i}(k))f_{p,i}(k) \\
 n_{p,i}^a(k+1) &= n_{p,i}^a(k) + \alpha_{p,i-1}(k)f_{p,i-1}(k) - \alpha_{p,i}(k)f_{p,i}(k) \\
 n_{p,i}(k+1) &= n_{p,i}(k) + f_{p,i-1}(k) - f_{p,i}(k). \quad (3)
 \end{aligned}$$

Accidents. In order to evaluate the performance of the developed RL policy in reacting to disturbances, we consider stochastic accidents occurring in the network. We model traffic accidents as stochastic events, each of which causes one lane to be closed. We let accidents occur in any cell at any time with equal probability. Each accident is cleared out after some number of time steps, which is drawn from a Poisson distribution. If $\bar{b}_{p,i}$ lanes of cell i of path p are closed due to accidents, then the jam density and the critical density for the cell reduce to $(b_{p,i} - \bar{b}_{p,i})/b_{p,i}$ of their original values. Hence, accidents introduce time-dependency to critical density and jam density variables.

III. NETWORK DYNAMICS: ROUTING FOR HUMANS AND AUTONOMOUS VEHICLES

We consider a network of P parallel paths and use $[P]$ to denote the set of paths. We use λ^h and λ^a to denote the human-driven and autonomous vehicle demands, respectively. As the number of vehicles entering a road is limited by the *supply* of the first cells, we model cars desiring to enter the network as forming a queue q that consists of packets each holding q_j cars. We provide a mathematical description of how this queue disburses cars into the network in the Appendix (Section VII-B).

A. Human choice dynamics

In general, people wish to minimize the amount of time spent traveling. However, people don't change routing choices instantaneously in response to new information; rather they have

some inertia and only change strategies sporadically. Moreover, we assume people only account for current conditions and do not strategize based on predictions of the future [28]. Accordingly, we use an *evolutionary dynamic* to describe how a population of users choose their routes. Specifically, we model the human driver population as following Hedge Dynamics, also called Log-linear Learning [29]–[31].

Let $\mu^h \in \mathbb{R}_{\geq 0}^P$ be the *routing vector* for the human-driven flow, where μ_p^h represents the fraction of human-driven vehicles that choose to travel on path p ; accordingly, $\sum_{p \in [P]} \mu_p^h = 1$. Let $\ell_p(k)$ denote how long it would take to traverse path p if a user starts at time k ; our model assumes that users have an accurate assessment of this delay, which is plausible given the widespread use of navigation services such as Google Maps or Waze. The routing vector is updated as follows.

$$\mu_p^h(k+1) = \frac{\mu_p^h(k) \exp(-\eta^h(k)\ell_p(k))}{\sum_{p' \in [P]} \mu_{p'}^h(k) \exp(-\eta^h(k)\ell_{p'}(k))}. \quad (4)$$

The ratio of the volume of vehicles using a road at successive time steps is inversely proportional to the exponential of the delay experienced by users of that road. The learning rate $\eta^h(k)$ may be decreasing or constant. Krichene *et al.* introduce this model in the context of humans' routing choices and simulate a congestion game with Amazon Mechanical Turk users to show the model accurately predicts human behavior [32].

B. Autonomous vehicle control policy

We assume that we have control over the routing of autonomous vehicles. We justify this by assuming that a city can coordinate with the owner of an autonomous fleet to decrease congestion in the city. Moreover, unlike traditional tolling, coordination between autonomous vehicles and city infrastructure makes it possible to have fast-changing and geographically finely quantized tolls, allowing routing control to be achieved through incentives [33]. The routing of autonomous vehicles is then our control parameter by which we influence the state of traffic on the network. We denote the autonomous routing vector $\mu^a \in \mathbb{R}_{\geq 0}^P$, where $\sum_{p \in [P]} \mu_p^a = 1$.

We assume the existence of a central controller, or social planner, which dictates μ^a by processing the state of the network. At each time step, we let the controller observe:

- the number of human-driven and autonomous vehicles in each cell,

- the total number of human-driven and autonomous vehicles waiting in the queue, and
- binary states for each lane that indicates whether the lane is closed due to an accident or not.

We use deep RL to arrive at a policy for the social planner to control the autonomous vehicle routing, μ^a . Since the state space is very large and both state and action spaces are continuous, a dynamic programming-based approach is infeasible. For instance, even if we discretized the spaces, say with 10 quantization levels, and did not have accidents, we would have 10^{82} possible states, and 10 actions for a moderate-size network with 40 cells in total.

We wish to minimize the total latency experienced by users, which is equal to summing over time the number of users in the system at each time step. Accordingly, we consider the following stage cost:

$$J(k) = \sum_j q_j(k) + \sum_{p \in [P]} \sum_{i \in [I_p]} n_{p,i}(k) \quad (5)$$

Due to their high performance in continuous control tasks [7], [34], we employ policy gradient methods to come up with a policy that produces μ^a given the observations. Specifically, we use state-of-the-art PPO with an objective function augmented by adding an entropy bonus for sufficient exploration [7], [35]. We build a deep neural network, and train it using Adam optimizer [36]. The set of parameters we use is in the Appendix (Section VII-E). We set each episode to have a fixed number of time steps.

In order to evaluate the performance of our control policy, we use three criteria. The first is the *throughput* of the network – we wish to have a policy that can serve any feasible demand, thereby stabilizing the queue. The second is the *average delay* experienced by users of the network, which we measure by counting the number of vehicles in the system. The third is the *convergence* to some steady state; we wish to avoid wild oscillations in congestion. To contextualize the performance of our control policy in this framework, we first establish the performance of *equilibria* of the network.

IV. EQUILIBRIUM ANALYSIS

In this section, we examine the possible *equilibria* of our dynamical system, which characterize the possible steady state behaviors of the system. A network with a given demand can have a variety of equilibria with varying average user delay. If our control achieves overall delay equal to that of the best possible equilibrium, it is a successful policy. Section V shows that our learned policy can achieve the best equilibrium in a variety of settings.

We are interested in network equilibria, which require both equilibrium on each path as well as equilibrium with respect to the human choice dynamics. Equilibria are parameterized by vehicle flow demand. Hence, we assume for theoretical analysis that the flow demands are constant and there are no accidents. In this section we provide sketches of proofs for the theoretical results and defer the full proofs, including proofs of the lemmas, to the appendix. We first analyze path equilibria.

A. Path equilibrium

To ease our analysis, we begin by restricting the considered class of roads to those with a single bottleneck, meaning one point on the road at which cell capacity drops. Formally, we consider each path p to have m_p^n cells, each with b_p^n lanes, followed by m_p^b cells downstream, each with b_p^b lanes, where $b_p^b < b_p^n$. We define $r_p := b_p^b/b_p^n \in (0, 1)$.

Assumption 1. *All cells in a path have the same model parameters, except for a decrease in the number of cell lanes after the m_p^n upstream-most cells.*

We use \bar{v}_p to denote the free-flow velocity of path p . Using Assumption 1, we present a theoretical result that completely analytically characterizes the road latencies that can occur at equilibrium.

Theorem 1. *At equilibrium, a road p with flow dynamics described by (3) will have the same autonomy level in all cells. Denote this autonomy level α_p . Under Assumption 1, if the vehicle flow demand is strictly less than the minimum cell capacity, the road will have no congested cells. Otherwise, the road will have any of the following latencies, where $\gamma_p \in \{0, 1, 2, \dots, m_p^n\}$:*

$$\ell_p = \frac{I_p}{\bar{v}_p} + \gamma_p \frac{(1 - r_p) \bar{n}_p^n (\alpha_p h_p^a + (1 - \alpha_p) h_p^h)}{r_p \bar{v}_p b_p^n}.$$

Proof. The proof is composed of three lemmas. We first establish a property of road equilibria that allows us to treat the vehicle flow as if it were composed of a single car type. With this, we use the CTM model to characterize possible equilibria on a road. We then derive the delay associated with each congested cell. Combining the latter two lemmas yields the theorem. We begin with a lemma based on the definition of equilibrium, in which there is constant incoming flow of each car type.

Lemma 1. *A path in equilibrium with nonzero incoming flow has the same autonomy level in all cells of the road, which is equal to the autonomy level of the vehicle flow onto the road. Formally, a path p with demand $(\bar{\lambda}_p^h, \bar{\lambda}_p^a)$ in equilibrium has*

$$\alpha_{p,1} = \alpha_{p,2} = \dots = \alpha_{p,I_p} = \bar{\lambda}_p^a / (\bar{\lambda}_p^h + \bar{\lambda}_p^a).$$

With this result, our analysis of road equilibria simplifies to that of single-typed traffic, with the autonomy level treated as a parameter. The next lemma, similarly to Theorem 4.1 of [6], completely characterizes the congestion patterns that can occur in road equilibria.

Lemma 2. *Under Assumption 1, if the demand on a road is less than the minimum capacity of its cells, they will be uncongested at equilibrium. Otherwise, a road with demand equal to the minimum cell capacity will have m_p^n equilibria. The set of equilibria has the following congested cells:*

$$\{\emptyset, \{m_p^n\}, \{m_p^n - 1, m_p^n\}, \dots, \{1, \dots, m_p^n - 2, m_p^n - 1, m_p^n\}\}.$$

We use these properties to find a closed-form expression for the latency incurred by traveling through a bottleneck cell, which when combined with Lemma 2, completes the proof.

Lemma 3. *The latency incurred by traveling through a congested cell is as follows.*

$$\frac{1}{\bar{v}_p} + \frac{(1 - r_p)\bar{n}_p^n(\alpha_p h_p^a + (1 - \alpha_p)h_p^h)}{r_p \bar{v}_p b_p^n}. \quad \square$$

The two terms above are the free-flow delay and the per-cell latency due to congestion, respective. Theorem 1 allows us to calculate the possible latencies of a road as a function of its autonomy level α_p . Since in a network equilibrium all used roads have the same latency, we can calculate network equilibria more efficiently than comprehensively searching over all possible routings. However, the discretization of roads into cell poses a problem – if cells are too big a network equilibrium may not even exist! To avoid this artifact from modeling with CTM, when analyzing network equilibria we consider the cells to be small enough that we can consider the continuous variable $\gamma_p \in [0, m_p^n]$.

B. Network equilibrium

We define the best equilibrium to be the equilibrium that serves a given flow demand with minimum latency. We are now ready to establish properties of network equilibria, as well as how to compute the best equilibria. We use the following two assumptions in our analysis of network equilibrium.

Assumption 2. *No two paths have the same free-flow latency.*

Assumption 3. *The initial choice distribution has positive human-driven and autonomous vehicle flow on each road.*

We use the convention of ordering the roads in the order of increasing free-flow latency.

Theorem 2. *Under Assumptions 1 and 2, a routing that minimizes total latency when all users (both human drivers and autonomous users) are selfish can be computed in $O(P^3 \log P)$ time. A routing that minimizes total latency when human drivers are selfish and autonomous users are controlled can also be computed in $O(P^3 \log P)$ time.*

Proof. We first establish properties of network equilibria.

Lemma 4. *Under Assumption 2, if some users are selfish and some users are not selfish, then the best equilibrium will have the following properties:*

- 1) *the road with largest free-flow latency used by selfish users will be in free-flow,*
- 2) *all roads with lower free-flow latency will be congested,*
- 3) *roads with greater free-flow latency may have nonselfish users, and*
- 4) *roads used with larger free-flow latency that have nonselfish users on them will be at capacity, except perhaps the road with largest free-flow latency that is used by nonselfish users.*

Using these theoretical results, optimal equilibria can be calculated efficiently using the linear programs described in the Appendix. \square

Using these properties to compute optimal equilibria as in the Appendix (Section VII-D), we establish a framework for

understanding the performance of our learned control policy. If the policy can reach the best equilibrium latency starting from arbitrary road conditions we view the policy as successful. We use this baseline to evaluate our experimental results in the following section.

A question then arises: if we have computed the best possible equilibria, why don't we directly implement that control? This approach is not fruitful, since the network can start in any state, including worse equilibria, from which good equilibria won't emerge when autonomous vehicles unilaterally use their routing in the best equilibrium. A dynamic policy which depends on the current traffic state is therefore needed to guide the network to the best equilibrium. As shown in the following, the learned policy reaches the best equilibrium in a variety of settings.

V. EXPERIMENTS AND RESULTS

In all of the experiments², we adopt the following parameters. All vehicles are 4 meters long. Human drivers keep a 2 second headway distance, whereas autonomous cars can keep 1 second. Each time step corresponds to 1 minute of real-life simulation. Each episode during deep RL training covers 5 hours of real-life simulation (300 time steps). In test time, we simulate 6 hours of real-life (360 time steps). We divide roads into the cells such that it takes 1 time step to traverse each cell in free-flow. We initialize $n_{p,i} \sim \text{unif}(0, \bar{n}_{p,i})$ for $\forall i \in [I_p], p \in [P]$.

Our overall control scheme can be seen in Fig. 1(a). As the learning model, we build a two-hidden-layer neural network, with each layer having 256 nodes. We train an RL agent for each configuration that we will describe later on. All trainings simulate 40 million time steps³.

We compare our method with a baseline where all cars are selfish and use the human choice dynamics presented in Sec. III-A. In all experiments, we set $\eta^h(k)$ (and $\eta^a(k)$ for the baseline) to be $0.5 \forall k$.

We consider a network from downtown Los Angeles to the San Fernando Valley with 3 roads. The highway numbers and the approximated parameter tuples (length, number of lanes, speed limit) are:

- 1) 110N (5 miles, 3 lanes, 60 mph); 101N (10 miles, 3 lanes for 5 miles then 2 lanes, 60 mph)
- 2) 10E (5 miles, 4 lanes, 75 mph); 5N (10 miles, 4 lanes, 75 mph); 134W (5 miles, 3 lanes, 75 mph)
- 3) 10W; 405N (both 10 miles, 4 lanes, 75 mph); 101S (5 miles, 3 lanes, 75 mph)

We perform three sets of experiments. In the first two, we disable accidents and set demand variance 0, i.e. $\lambda^a = \bar{\lambda}^a$, $\lambda^h = \bar{\lambda}^h$ to have no perturbations after initialization.

Varying number of roads. In the first set, we vary the number of routes $P \in \{2, 3, 4\}$ by duplicating, or removing, the third route. We set the autonomy level of the demand $\bar{\alpha} = 0.6$, and $\bar{\lambda}^h + \bar{\lambda}^a$ to be 95% of the maximum capacity under this autonomy level. We plot learning curves in Fig. 4 (a). It can be seen that even with $P=4$ when observation space is 144-dimensional (as the accidents were disabled), the agent successfully learns routing within 40 million time steps. With randomized initial states, the agents learn routing policies that

²We make the code available in the supplementary material.

³Other hyperparameter values we use for PPO are in the Appendix.

achieve nearly as good as optimal equilibrium when $P \in \{2, 3\}$. While the agent for $P=4$ also decreases the average cost, it requires either a little more training, or better hyperparameter tuning. In Fig. 4 (b), we plot the number of cars (mean \pm standard error over 100 simulations) in the system as a function of time steps. While selfish routing causes congestion by creating linearly growing queues when $P > 2$, RL policies successfully stabilize queues and even reach car numbers of optimal equilibria when $P < 4$. From the learning curve for $P=4$, it can be deduced we can also achieve car numbers of optimal equilibria with more careful training.

Varying autonomy. We take $P=3$ and vary the autonomy of demand $\bar{\alpha} \in \{0.4, 0.5, 0.6, 0.7\}$ without changing the total demand $\bar{\lambda}^h + \bar{\lambda}^a$. Note the demands are infeasible when $\bar{\alpha} \in \{0.4, 0.5\}$. In Fig. 5 (a), we plot the number of cars (mean \pm standard error over 100 simulations) in the system as a function of time steps. The result is similar to the previous experiment when the demand is feasible. With infeasible demand, RL agent keeps a queue that is only marginally longer than the queue that would be created by optimal equilibrium. On the other hand, selfish routing grows the queue with much faster rates. These experiments show RL policy successfully handles random initializations.

Perturbations. In the third set, we fix $P=3$ and $\bar{\alpha}=0.6$ for the same total average demand. We evaluate what happens when we enable accidents and noise in the demand. We assume the standard deviations of the demand noise are $\bar{\lambda}^h/10$ and $\bar{\lambda}^a/10$ for human-driven and autonomous vehicles, respectively. We set the probability of accidents such that the expected frequency of accidents is 1 per 100 minutes, and clearing out an accident takes 30 minutes on average [37]. As it can be seen from Fig. 5 (b), the RL agent successfully handles the perturbations due to accidents and noisy demands. This plot also shows how accidents perturb the system. To give a clearer picture, we provide detailed information about the system states in Fig. 6, which shows the number of cars in each cell as well as the queue lengths over time. The small oscillations, which occur even after the effect of the accidents disappear (after fifth hour), are due to noisy demand and the discretization of cells. With selfish routing, the vehicles tend to not use the longest road. They use it only when there is an accident in another road (around first hour) or the other two roads are congested (around fourth hour). In contrast, RL makes good use of the network and leads to altruistic behavior. It also handles the accidents by effectively altering the routing of autonomous cars (around fourth hour, autonomous cars start using the first route until the accident is cleared). Hence, it manages to stabilize the queue and prevent congestion. We provide video visualizations of this run in the supplementary material.

VI. CONCLUSION

Summary. In this work we presented a framework for understanding a dynamic traffic network shared between selfish human drivers and controllable autonomous vehicles. We show, using reinforcement learning, we can find a policy to minimize the average travel time experienced by users of the network. We develop theoretical results to describe and calculate the best equilibria that can exist and show that our policy reaches the best possible equilibrium performance. Further, we provide

case studies showing how the training period scales with the number of roads, and we show that our control policy is robust to accidents and stochastic demand.

Limitations. We used the number of cars in each cell as predictive features for RL training. Although this makes the state space dimensionality grow only linearly with the number of cells, it may not be scalable to much larger traffic networks.

Future work. This work opens up many future directions for research, including improving how the training time scales with the number of roads and extending this to more complex network topologies.

ACKNOWLEDGMENT

The authors would like to thank Kenneth Wang for creating the video visualizations of the project. Toyota Research Institute (TRI) provided funds to assist the authors with their research but this article solely reflects the opinions and conclusions of its authors and not TRI or any other Toyota entity

REFERENCES

- [1] D. Schrank, B. Eisele, T. Lomax, and J. Bak, "Urban mobility scorecard," 2015.
- [2] A. Henao, *Impacts of Ridesourcing-Lyft and Uber-on Transportation Including VMT, Mode Replacement, Parking, and Travel Behavior*. University of Colorado at Denver, 2017.
- [3] T. Roughgarden and É. Tardos, "How bad is selfish routing?" *Journal of the ACM (JACM)*, 2002.
- [4] W. Hu, "Over \$10 to drive in manhattan? what we know about the congestion pricing plan," *The New York Times*, 2019.
- [5] X.-Y. Lu, P. Varaiya, R. Horowitz, D. Su, and S. E. Shladover, "Novel freeway traffic control with variable speed limit and coordinated ramp metering," *Transportation Research Record*, 2011.
- [6] G. Gomes, R. Horowitz, A. A. Kurzhanskiy, P. Varaiya, and J. Kwon, "Behavior of the cell transmission model and effectiveness of ramp metering," *Transportation Research Part C: Emerging Technologies*, 2008.
- [7] J. Schulman, F. Wolski, P. Dhariwal, A. Radford, and O. Klimov, "Proximal policy optimization algorithms," *Preprint, arXiv:1707.06347*, 2017.
- [8] W. Krichene, J. D. Reilly, S. Amin, and A. M. Bayen, "Stackelberg routing on parallel transportation networks," *Handbook of Dynamic Game Theory*.
- [9] E. Bıyık, D. A. Lazar, R. Pedarsani, and D. Sadigh, "Altruistic autonomy: Beating congestion on shared roads," in *Workshop on the Algorithmic Foundations of Robotics*, 2018.
- [10] C. F. Daganzo, "The cell transmission model: A dynamic representation of highway traffic consistent with the hydrodynamic theory," *Transportation Research Part B: Methodological*, 1994.
- [11] S. C. Dafermos, "The traffic assignment problem for multiclass-user transportation networks," *Transportation science*, 1972.
- [12] D. W. Hearn, S. Lawphongpanich, and S. Nguyen, "Convex programming formulations of the asymmetric traffic assignment problem," *Transportation Research Part B: Methodological*, 1984.
- [13] D. A. Lazar, S. Coogan, and R. Pedarsani, "Routing for traffic networks with mixed autonomy," *arXiv preprint arXiv:1809.01283*, 2018.
- [14] N. Mehr and R. Horowitz, "Can the presence of autonomous vehicles worsen the equilibrium state of traffic networks?" in *Conference on Decision and Control*. IEEE, 2018.
- [15] J. Lazarus, J. Ugrumurera, S. Hinardi, M. Zhao, F. Shyu, Y. Wang, S. Yao, and A. M. Bayen, "A decision support system for evaluating the impacts of routing applications on urban mobility," in *21st International Conference on Intelligent Transportation Systems*. IEEE, 2018.
- [16] M. Wu, S. Amin, and A. E. Ozdaglar, "Value of information systems in routing games," *arXiv preprint arXiv:1808.10590*, 2018.
- [17] T. Roughgarden, "Stackelberg scheduling strategies," *SIAM Journal on Computing*, 2004.
- [18] C. Swamy, "The effectiveness of stackelberg strategies and tolls for network congestion games," *ACM Transactions on Algorithms*, 2012.
- [19] W. Krichene, M. S. Castillo, and A. Bayen, "On social optimal routing under selfish learning," *IEEE Transactions on Control of Network Systems*, 2018.

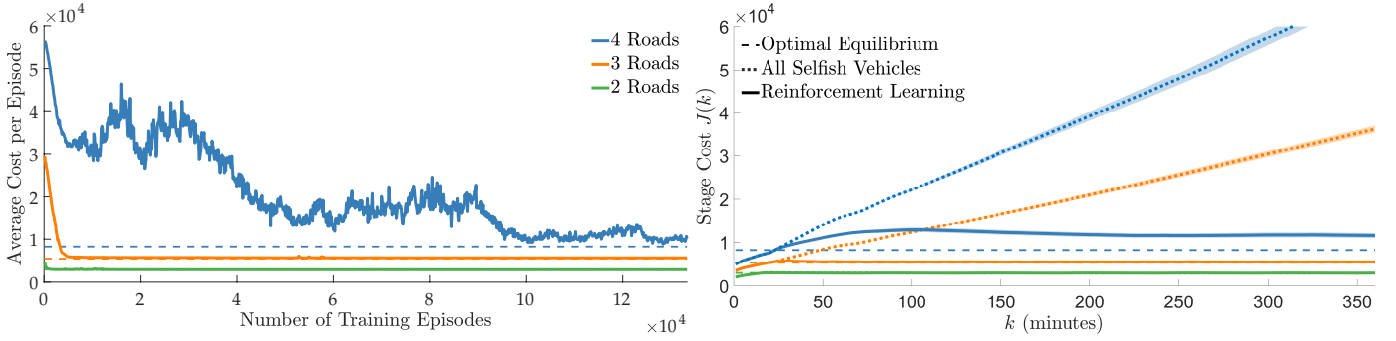


Fig. 4: Varying number of roads. (a) Average number of cars in the system per episode during RL training. (b) Time vs. number of cars in the system for the comparison of selfish and RL routing.

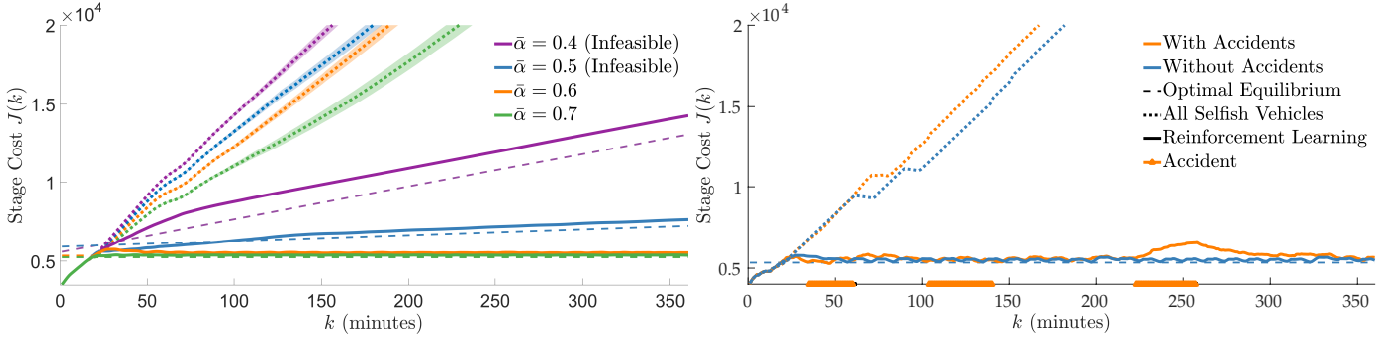


Fig. 5: (a) Varying autonomy. (b) Varying the presence of accidents and noise in the demand.

- [20] A. Muralidharan, G. Dervisoglu, and R. Horowitz, “Freeway traffic flow simulation using the link node cell transmission model,” in *American Control Conference*. IEEE, 2009.
- [21] S. Cui, B. Seibold, R. Stern, and D. B. Work, “Stabilizing traffic flow via a single autonomous vehicle: Possibilities and limitations,” in *Intelligent Vehicles Symposium*. IEEE, 2017.
- [22] C. Wu, A. M. Bayen, and A. Mehta, “Stabilizing traffic with autonomous vehicles,” in *International Conference on Robotics and Automation*, 2018.
- [23] F. Belletti, D. Haziza, G. Gomes, and A. M. Bayen, “Expert level control of ramp metering based on multi-task deep reinforcement learning,” *IEEE Transactions on Intelligent Transportation Systems*, 2018.
- [24] M. A. Wright, S. F. Ehlers, and R. Horowitz, “Neural-attention-based deep learning architectures for modeling traffic dynamics on lane graphs,” *arXiv preprint arXiv:1904.08831*, 2019.
- [25] A. Askari, D. A. Farias, A. A. Kurzhanskiy, and P. Varaiya, “Effect of adaptive and cooperative adaptive cruise control on throughput of signalized arterials,” in *Intelligent Vehicles Symposium*. IEEE, 2017.
- [26] D. Lazar, S. Coogan, and R. Pedarsani, “Capacity modeling and routing for traffic networks with mixed autonomy,” in *56th Annual Conference on Decision and Control*. IEEE, 2017.
- [27] D. A. Lazar, R. Pedarsani, K. Chandrasekher, and D. Sadigh, “Maximizing road capacity using cars that influence people,” in *Conference on Decision and Control*. IEEE, 2018.
- [28] W. H. Sandholm, *Population games and evolutionary dynamics*. MIT press, 2010.
- [29] N. Cesa-Bianchi and G. Lugosi, *Prediction, learning, and games*. Cambridge university press, 2006.
- [30] J. R. Marden and J. S. Shamma, “Revisiting log-linear learning: Asynchrony, completeness and payoff-based implementation,” *Games and Economic Behavior*, 2012.
- [31] L. E. Blume, “The statistical mechanics of strategic interaction,” *Games and economic behavior*, 1993.
- [32] W. Krichene, M. C. Bourguiba, K. Tlam, and A. Bayen, “On learning how players learn: Estimation of learning dynamics in the routing game,” *Transactions on Cyber-Physical Systems*, 2018.
- [33] E. Bityk, D. A. Lazar, D. Sadigh, and R. Pedarsani, “The green choice: Learning and influencing human decisions on shared roads,” *arXiv preprint arXiv:1904.02209*, 2019.
- [34] J. Schulman, S. Levine, P. Abbeel, M. Jordan, and P. Moritz, “Trust region policy optimization,” in *International Conference on Machine Learning*, 2015.
- [35] V. Mnih, A. P. Badia, M. Mirza, A. Graves, T. Lillicrap, T. Harley, D. Silver, and K. Kavukcuoglu, “Asynchronous methods for deep reinforcement learning,” in *International conference on machine learning*, 2016.
- [36] D. P. Kingma and J. Ba, “Adam: A method for stochastic optimization,” *Preprint, arXiv:1412.6980*, 2014.
- [37] H. TranStar, “2017 annual report,” Houston TranStar, Report, 2018, accessed: January 28, 2019. [Online]. Available: http://houstontranstar.org/about_transtar/docs/Annual_2017_TransTar.pdf

VII. APPENDIX

A. Summary of notation

See Table I.

B. Queue dynamics

We consider a queue of vehicles that are waiting to join the network. In order to describe the dynamics of the queue we borrow the “packet” terminology from communication networks. We consider a packet of vehicles to be a tuple (q_j^h, q_j^a) , where $q_j^h \in \mathbb{R}_{\geq 0}$ is a volume of human-driven vehicles and $q_j^a \in \mathbb{R}_{\geq 0}$ is a volume of autonomous vehicles. At each time step a nonnegative random demand $(\lambda^h(k), \lambda^a(k))$ is added as a packet to the end of the queue, and vehicles enter the network starting from the front of the queue, starting with the zeroth packet. This structure preserves the first-in-first-out property for the network.

The factor limiting vehicles from entering the network is the supply on each road, $(\bar{n}_{p,1} - n_{p,1}(k))w_{p,1}(\alpha_{p,1}(k))$. We allocate as many packets, and fractions of packets, as possible until the supply constraint is violated on one of the roads. Formally, at each time step the queue is updated as in

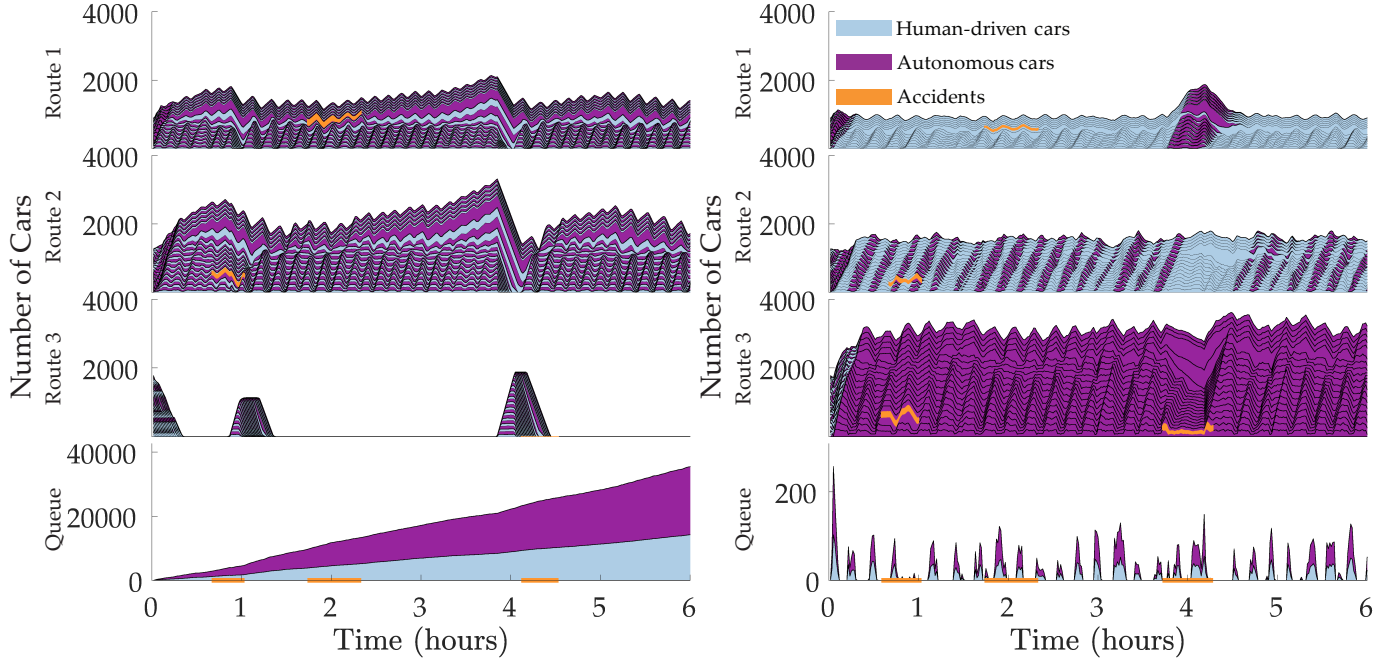


Fig. 6: The network under perturbations due to accidents and noisy demand. For each road and time step, from bottom to top, the stacked color segments show the number of cars in the cells from origin to the destination. Congestion occurs only upstream to the bottlenecks. (a) Selfish routing. (b) RL routing.

TABLE I: Summary of Notation

p	Path, or road, index	unitless
P	# of paths in the network	paths
$[P]$	Set of paths in the network	set of paths
i	Cell index	unitless
(p, i)	Cell i of path p	unitless
I_p	# of cells in path p	cells
(q_j^h, q_j^a)	# of vehicles in queue packet j	tuple of vehicles
$\bar{v}_{p,i}$	Free-flow velocity of (p, i)	cells/time step
$b_{p,i}$	Number of lanes of (p, i)	unitless
$h_{p,i}^h (h_{p,i}^a)$	Nominal vehicle headway on (p, i)	cells/vehicle
$n_{p,i}^h (n_{p,i}^a)$	Density of vehicles on (p, i)	vehicles/cell
$n_{p,i}$	Total vehicle density on (p, i)	vehicles/cell
$f_{p,i}^h (f_{p,i}^a)$	Flow of vehicles from (p, i)	vehicles/time step
$f_{p,i}$	Total flow from (p, i) to $(p, i+1)$	vehicles/time step
$\alpha_{p,i}$	Autonomy level of (p, i)	unitless
$\bar{n}_{p,i}(\alpha)$	Critical density of (p, i) , at aut. α	vehicles/cell
$\bar{n}_{p,i}$	Jam (maximum) density of (p, i)	vehicles/cell
$\bar{F}_{p,i}(\alpha)$	Capacity of (p, i) , at aut. α	vehicles/time step
$w_{p,i}(\alpha)$	Shockwave speed of (p, i) , at aut. α	cells/time step
k	Time index	unitless
$\ell_p(k)$	Latency of path p if starting at time k	time steps
$\mu^h (\mu^a)$	Routing vector	unitless
$J(k)$	Stage cost at time k	vehicles
$m_p^b (m_p^a)$	# of (non)bottleneck cells on path p	cells
$b^b (b^a)$	# of lanes in (non)bottleneck cells on p	unitless
r_p	$:= b^b/b^a$	unitless
γ_p	Number of congested cells on path p	cells

Algorithm 1 Queue Dynamics

Append packet $(\bar{\lambda}^h(k), \bar{\lambda}^a(k))$ to the end of the queue
 $f^h \leftarrow \mathbf{0}_P, f^a \leftarrow \mathbf{0}_P$
 $s_p \leftarrow (\bar{n}_{p,1} - n_{p,1}(k))w_{p,1}(\alpha_{p,1}(k)) \quad \forall p \in [P]$
while $f_p^h + f_p^a < s_p \quad \forall p \in [P]$ **do**
 if $f_p^h + f_p^a + \mu^h(k)q_0^h + \mu^a(k)q_0^a \leq s_p \quad \forall p \in [P]$ **then**
 $f_p^h \leftarrow f_p^h + q_0^h \quad \forall p \in [P]$
 $f_p^a \leftarrow f_p^a + q_0^a \quad \forall p \in [P]$
 Update state of the queue
 if queue empty **then**
 break
 end if
 else
 $y^* \leftarrow \arg \max_{y \in [0,1]} y$
 s.t. $f_p^h + f_p^a + y(\mu^h(k)q_0^h + \mu^a(k)q_0^a) \leq s_p, \forall p \in [P]$
 $f_p^h \leftarrow f_p^h + y^* q_0^h \quad \forall p \in [P]$
 $f_p^a \leftarrow f_p^a + y^* q_0^a \quad \forall p \in [P]$
 $q_0^h \leftarrow (1 - y^*)q_0^h$
 $q_0^a \leftarrow (1 - y^*)q_0^a$
 break
 end if
end while

Algorithm 1, where $\mathbf{0}_P$ denotes the P -dimensional zero vector.

C. Proofs for Section IV-A

Proof of Lemma 1

Proof. By definition, at equilibrium, the number of vehicles in each cell i of road p , $n_{p,i}^a(k)$ and $n_{p,i}^h(k)$ is constant for all times k . Since by definition the incoming flow is also

constant, by (2), a constant state implies constant flows. By (3), a constant density also implies that the incoming and outgoing flow in each cell are equal. This means that all cells will have the same incoming flow as the first cell. Further, we know that since the density of autonomous vehicles is constant over time, incoming and outgoing autonomy levels are equal, *i.e.* $\alpha_{p,i-1}(k)f_{p,i-1}(k) = \alpha_{p,i}(k)f_{p,i}(k)$. Since we also have $f_{p,i-1}(k) = f_{p,i}(k)$, this implies that $\alpha_{p,i-1}(k) =$

$\alpha_{p,i}(k)$. Therefore the autonomy level of all cells is the same. Let us denote this uniform autonomy level α_p . For the first cell, $\bar{\lambda}_p^h + \bar{\lambda}_p^a = f_{p,0}$ and $\bar{\lambda}_p^a = \alpha_p f_{p,0}$. Combining these two expressions, we find $\alpha_p = \bar{\lambda}_p^a / (\bar{\lambda}_p^h + \bar{\lambda}_p^a)$. \square

Proof of Lemma 2

Proof. As mentioned in Section IV-A, this lemma relates closely to Theorem 4.1 of [6]. However, we cannot directly apply that theorem due to differing assumptions; namely they assume $\bar{F}_{i+1} = (\bar{n}_i - \tilde{n}_i)w_i \forall i$. We therefore offer a similar proof, tailored to our assumptions.

For ease of notation, we drop all path subscripts p as well as the cell index for the free-flow velocity parameter \bar{v} . In light of Lemma 1, we also suppress the autonomy level arguments to capacity \bar{F}_i and critical density \tilde{n}_i . The flow equation then becomes $f_i = \min(\bar{v}n_i, (\bar{n}_{i+1} - n_{i+1})w_{i+1}, \bar{F}_i)$.

We begin by proving that if the vehicle flow demand is strictly less than the minimum capacity, *i.e.* the bottleneck capacity, then the only equilibrium has no congested cells. As mentioned in Section II, in our model there is no supply limit to the flow exiting a road, so $f_I = \min(\bar{v}n_I, \bar{F}_I)$. Since $f_0 = f_I < \bar{F}_I$, $f_0 = f_I = \bar{v}n_I$. The definition of capacity, $\bar{F}_i = \bar{v}\tilde{n}_i$, then implies that $n_I < \tilde{n}_I$, meaning that cell I is uncongested, so $\bar{v}n_I < (\bar{n}_I - n_I)w_I$.

This is the base case for a proof by induction. Consider cell i that is uncongested (*i.e.* $n_i < \tilde{n}_i$). Since by assumption all cells have flow strictly less than the cell's capacity, $f_i = \bar{v}n_i < \bar{F}_i$. Then consider the flow entering cell i : $f_{i-1} = \min(\bar{v}n_{i-1}, (\bar{n}_i - n_i)w_i, \bar{F}_{i-1}) = f_i < \bar{F}_i < (\bar{n}_i - n_i)w_i$.

The fact that $\bar{F}_i \leq \bar{F}_{i-1}$ then implies that $f_{i-1} = \bar{v}n_{i-1}$, so cell $i-1$ is uncongested, proving the lemma's first statement.

The second statement assumes that the flow on the path is equal to the minimum capacity. The cells in the bottleneck segment all have the same capacity, which we denote \bar{F}^b ; this capacity is less than the capacity of the cells in the nonbottleneck segment. This means that all bottleneck cells will be operating at capacity (and therefore have vehicle density equal to their critical density); flow on the road is therefore equal to \bar{F}^b .

We now turn to the nonbottleneck segment. We first note that if a nonbottleneck cell is uncongested then the preceding cell must be uncongested as well, using the same reasoning as that proving the first statement above. Next, consider the flow out of the downstream-most cell of the nonbottleneck segment: $f_{m^n} = \min(\bar{v}n_{m^n}, (\bar{n}_{m^n+1} - n_{m^n+1})w_{m^n+1}, \bar{F}_{m^n}) = \bar{F}^b < \bar{F}_{m^n}$, so $f_{m^n} = \min(\bar{v}n_{m^n}, (\bar{n}_{m^n+1} - n_{m^n+1})w_{m^n+1})$. Cell m^n can be uncongested, in which case the cell density is such that $\bar{v}n_{m^n} = \bar{F}^b$, or the cell can be congested, in which case the second term dominates. Then, if nonbottleneck cell i is congested, the flow into it is $f_{i-1} = \min(\bar{v}n_{i-1}, (\bar{n}_i - n_i)w_i)$. Again, to achieve this flow, cell $i-1$ can be either congested or uncongested. As shown above, if $i-1$ is uncongested, then all upstream cells must be uncongested as well, yielding the second statement in the theorem. \square

Proof of Lemma 3

Proof. Recall that we assume roads have a uniform free-flow velocity across all cells in a road, where path p has free-flow velocity \bar{v}_p . We defined $[m_p^n]$ as the set of cells before the

bottleneck, which have b_p^n lanes. The remaining cells, with indices in the set $[I_p] \setminus [m_p^n]$, have b_p^b lanes. Further recall the definition $r_p = b_p^b/b_p^n$. Let $\bar{F}_p^n(\alpha_p)$ denote the capacity of the cells before the bottleneck of path p with autonomy level α_p and let $\bar{F}_p^b(\alpha_p)$ be the same for the bottleneck cell. Note that $\bar{F}_p^b(\alpha_p) = r\bar{F}_p^n(\alpha_p)$. Similarly, let $w_p^n(\alpha_p)$ and $w_p^b(\alpha_p)$ denote the shockwave speed for prebottleneck cells and bottleneck cell, respectively, on path p with autonomy level α_p , as with jam densities \bar{n}_p^n and \bar{n}_p^b and critical densities $\tilde{n}_p^n(\alpha_p)$ and $\tilde{n}_p^b(\alpha_p)$.

To help our analysis, we define the *congestion profile*.

Definition 1. A congestion profile of a road is a binary vector that has the same length as the number of cells in the road, where each entry corresponds to a cell. If a cell is congested, the corresponding entry is 1, otherwise it is 0. Formally, $s_p \in \{0, 1\}^{I_p}$

Lemma 2 establishes all possible congestion profiles that a road in equilibrium can experience. We now investigate how much delay each congestion profile induces on the road, parameterized by the autonomy level of the road. Let f_p denote the flow on path p at an equilibrium. By Lemma 2 and the definitions of r and capacity (1),

$$f_p = \bar{F}_p^b = r_p \bar{F}_p^n(\alpha_p) = r_p w_p^n(\alpha_p) (\bar{n}_p^n - \tilde{n}_p^n(\alpha_p)). \quad (6)$$

Let $n_p^c(\alpha_p)$ denote the vehicle density in a congested cell on path p , which we know must occur upstream of the bottleneck (Lemma 2). Then, the flow entering a congested cell before the bottleneck is $f_p = w_p^n(\alpha_p) (\bar{n}_p^n - n_p^c(\alpha_p))$. Equating this with (6), we find $n_p^c(\alpha_p) = (1 - r_p) \bar{n}_p^n + r_p \tilde{n}_p^n(\alpha_p)$.

To use this to find the latency incurred by traveling through a congested cell, we divide the density by the flow, as follows.

$$\begin{aligned} \frac{n_p^c(\alpha_p)}{f_p} &= \frac{n_p^c(\alpha_p)}{\bar{F}_p^b(\alpha_p)} = \frac{(1 - r_p) \bar{n}_p^n + r_p \tilde{n}_p^n(\alpha_p)}{r_p \bar{v}_p \tilde{n}_p^n(\alpha_p)} \\ &= \frac{1}{\bar{v}_p} + \frac{(1 - r_p) \bar{n}_p^n (\alpha_p h_p^a + (1 - \alpha_p) h_p^h)}{r_p \bar{v}_p b_p^n} \end{aligned}$$

D. Proofs for Section IV-B

We begin with a proposition which follows from the definition of equilibrium and Assumption 3.

Proposition 1. In a network equilibrium, the following are true.

- 1) All roads with selfish drivers have the same latency.
- 2) All roads without selfish drivers have equal or greater latency.

We next present a lemma that will support our results.

Lemma 5. If the set of equilibria contains a routing with positive flow only on roads $[p]$, then there exists a routing in the set of equilibria in which road p is in free-flow.

Proof. Under Assumption 2, no two roads have the same free-flow latency. With Proposition 1, this implies that if an equilibrium has a used road with no congestion, it must be the used road with greatest free-flow latency, as otherwise all used roads would not have the same latency. Therefore, if an equilibrium routing with positive flow on roads $[p]$ has a road in free-flow, it must be road p . Otherwise, we can construct an

equilibrium with the same demand that has road p in free-flow. Recall that the latency on roads in equilibrium is increasing with the length of the congested portion of the road, $\gamma_{p'}$, and $\gamma_{p'} = 0$ corresponds to an uncongested road. If all roads are congested, we consider decreasing the length of congestion on all roads simultaneously, at rates which keep the road latencies equal. This continues until road p becomes completely uncongested. This construction proves the lemma. \square

Proof of Lemma 4

Proof. The first property follows from Lemma 5, which proves the existence of such an equilibrium, which has overall latency less than that of an equilibrium with selfish users only on congested roads. The second property is from Proposition 1. The third property follows from the fact that we do not consider autonomous users to be selfish, and fourth properties result from our definition of the road latency function, which increases with congestion. \square

Proof of Theorem 2: computing equilibria

Proof. We denote the set of best equilibria for selfish human-driven and autonomous flow demand $\bar{\lambda}^h$ and $\bar{\lambda}^a$ as $\text{BNE}(\bar{\lambda}^h, \bar{\lambda}^a)$. We use $\hat{\ell}_p(\alpha_p)$ to denote the per-cell latency due to congestion, i.e. $\hat{\ell}_p(\alpha_p) = \frac{(1-r_p)\bar{n}_p^h(\alpha_p h_p^a + (1-\alpha_p)h_p^h)}{r_p \bar{v}_p b_p^a}$. Lemma 4 implies that for a given demand, all equilibria in the set $\text{BNE}(\bar{\lambda}^h, \bar{\lambda}^a)$ have one road that is in free-flow. We can then formulate the search for a best equilibrium as an optimization. We are helped by the fact that the best equilibria will use the minimum number of feasible roads, since all users experience the same delay. Then, for each candidate free-flow road (denote with index p'), check feasibility of only using roads $[p']$, and choose a routing that minimizes p' . The feasibility can be checked as follows, with an optimization that utilizes Lemma 4.

$$\begin{aligned} & \arg \min_{f^h \in \mathbf{R}_{\geq 0}^{p'}, f^a \in \mathbf{R}_{\geq 0}^{p'}, \gamma \in \prod_{p \in [p'-1]} [0, m_p^a]} 1 \\ \text{s.t. } & \gamma_p \hat{\ell}_p\left(\frac{f_p^a}{f_p^h + f_p^a}\right) = I_{p'}/\bar{v}_{p'} - I_p/\bar{v}_p, \forall p \in [p' - 1] \\ & \sum_{p \in [p']} f_p^h = \bar{\lambda}^h \\ & \sum_{p \in [p']} f_p^a = \bar{\lambda}^a \\ & f_{p'}^h + f_{p'}^a \leq \bar{F}_{p'}\left(\frac{f_{p'}^a}{f_{p'}^h + f_{p'}^a}\right) \\ & f_p^h + f_p^a = \bar{F}_p\left(\frac{f_p^a}{f_p^h + f_p^a}\right), \forall p \in [p' - 1] \end{aligned} \quad (7)$$

The last constraint yields an affine relationship between f_p^h and f_p^a for paths $p \in [p' - 1]$. Solving for f_p^h and plugging into the first constraint yields an affine relationship between γ_p and f_p^a . This way, the optimization can be converted to a linear program, and we must solve $\log P$ linear programs to search the minimum feasible p' .

This formulation assumes that all vehicles are selfish. If instead we consider selfish human drivers and fully controlled autonomous users, we can construct a similar optimization to

find the best equilibrium. For each choice of free-flow road p' , we minimize the total latency of the autonomous vehicles not on free-flow roads. We then choose the routing corresponding to free-flow road p' that minimizes total latency (which may not necessarily minimize the number of roads used by human drivers). For each candidate free-flow road p' we solve the following optimization.

$$\begin{aligned} & \arg \min_{f^h \in \mathbf{R}_{\geq 0}^{p'}, f^a \in \mathbf{R}_{\geq 0}^{P-p'}, \gamma \in \prod_{p \in [p'-1]} [0, m_p^a]} \sum_{p \in [P] \setminus [p']} f_p^a \frac{I_p}{\bar{v}_p} \\ \text{s.t. } & \gamma_p \hat{\ell}_p(\alpha_p) = I_{p'}/\bar{v}_{p'} - I_p/\bar{v}_p, \forall p \in [p' - 1] \\ & \sum_{p \in [p']} f_p^h = \bar{\lambda}^h \\ & \sum_{p \in [P]} f_p^a = \bar{\lambda}^a \\ & f_{p'}^h + f_{p'}^a \leq \bar{F}_{p'}\left(\frac{f_{p'}^a}{f_{p'}^h + f_{p'}^a}\right) \\ & f_p^h + f_p^a = \bar{F}_p\left(\frac{f_p^a}{f_p^h + f_p^a}\right), \forall p \in [p' - 1] \\ & f_p^a \leq \bar{F}^b(1), \forall p \in [P] \setminus [p']. \end{aligned} \quad (8)$$

This can be reformulated as a linear program by the same mechanism. Again, we solve $\log P$ linear programs and choose the one that corresponds to the minimum feasible p' . \square

E. Experiment details

In implementation, we used $J(k) - J(k-1)$ as a proxy cost for time step k , where $J(0) = 0$.

As the computation infrastructure, we used 2 different Ubuntu machines whose details are given below. For training we used 32 CPUs in each of them.

- Ubuntu 16.04, Intel[®] Xeon[®] Silver 4114 CPU @ 2.20GHz, 40 CPUs, 125GB RAM
- Ubuntu 18.04.2 LTS, Intel[®] Xeon[®] CPU @ 2.20GHz, 32 CPUs, 32GB RAM

Below are the set of hyperparameters that we used for Proximal Policy Optimization (PPO). We refer to [7] for the definitions of PPO-specific parameters. While this set yields good results as we presented in the paper, a careful tuning may improve the performance, especially when the number of roads P is large.

- Number of Time Steps: 40 million
- Number of Actors: 32 (32 CPUs in parallel)
- Time Steps per Episode During Training: 300
- Time Steps per Actor Batch: 1200
- ϵ for Clipping in the Surrogate Objective: 0.2
- Entropy Coefficient: 0.005
- Number of Optimization Epochs: 5
- Optimization Step Size: 3×10^{-4}
- Optimization Batch Size: 64
- γ for Advantage Estimation: 0.99
- λ for Advantage Estimation: 0.95
- ϵ for Adam Optimization: 10^{-5}
- Annealing for ϵ (Clipping) and Optimization Step Size: Linear (down to 0)